Macrophage Phenotype Controls Long-Term AKI Outcomes—Kidney Regeneration versus Atrophy

Maciej Lech,* Regina Gröbmayr,* Mi Ryu,* Georg Lorenz,* Ingo Hartter,* Shrikant R. Mulay,* Heni Eka Susanti,* Koichi S. Kobayashi,†‡ Richard A. Flavell,† and Hans-Joachim Anders*

*Division of Nephrology, Medical Clinic and Polyclinic IV, University of Munich, Munich, Germany; †Department of Immunobiology, Howard Hughes Medical Institute, Yale University School of Medicine, New Haven, Connecticut; and ‡Department of Microbial and Molecular Pathogenesis, Texas A&M Health Science Center, College Station, Texas

ABSTRACT

The mechanisms that determine full recovery versus subsequent progressive CKD after AKI are largely unknown. Because macrophages regulate inflammation as well as epithelial recovery, we investigated whether macrophage activation influences AKI outcomes. IL-1 receptor–associated kinase-M (IRAK-M) is a macrophage-specific inhibitor of Toll-like receptor (TLR) and IL-1 receptor signaling that prevents polarization toward a proinflammatory phenotype. In postischemic kidneys of wild-type mice, IRAK-M expression increased for 3 weeks after AKI and declined thereafter. However, genetic depletion of IRAK-M did not affect immunopathology and renal dysfunction during early postischemic AKI. Regarding long-term outcomes, wild-type kidneys regenerated completely within 5 weeks after AKI. In contrast, IRAK-M$^{-/-}$ kidneys progressively lost up to two-thirds of their original mass due to tubule loss, leaving atubular glomeruli and interstitial scarring. Moreover, M1 macrophages accumulated in the renal interstitial compartment, coincident with increased expression of proinflammatory cytokines and chemokines. Injection of bacterial CpG DNA induced the same effects in wild-type mice, and TNF-α blockade with etanercept partially prevented renal atrophy in IRAK-M$^{-/-}$ mice. These results suggest that IRAK-M induction during the healing phase of AKI supports the resolution of M1 macrophage– and TNF-α–dependent renal inflammation, allowing structural regeneration and functional recovery of the injured kidney. Conversely, IRAK-M loss-of-function mutations or transient exposure to bacterial DNA may drive persistent inflammatory mononuclear phagocyte infiltrates, which impair kidney regeneration and promote CKD. Overall, these results support a novel role for IRAK-M in the regulation of wound healing and tissue regeneration.

J Am Soc Nephrol 25: 292–304, 2014. doi: 10.1681/ASN.2013020152

As first described in 1967[1], AKI is now considered a predictor of subsequent CKD; however, the pathophysiologic mechanisms underlying this association remain largely unknown.[2–5] Ideally, 100% of nephrons regain their structural integrity and the functional capacity they had before AKI. However, assessing structural recovery is hardly feasible in clinical practice and assessing functional recovery by serum creatinine levels or GFR estimations is impossible, because any loss up to 40%–50% can be missed due to the lack of parameter sensitivity.[6–8] Thus, the clinical observation that AKI is often followed by CKD could simply result from incomplete AKI recovery, implying that AKI episodes involve some irreversible loss of nephrons due to insufficient repair.

What mechanisms regulate renal repair upon AKI? Whereas the limited capacity for podocyte regeneration (in adults) often limits glomerular repair, AKI usually involves tubular injury, which has a higher regenerative capacity.[9,10] There is

Received February 13, 2013. Accepted August 6, 2013.

M.L. and R.G. contributed equally to this work.

Published online ahead of print. Publication date available at www.jasn.org.

Correspondence: Dr. Maciej Lech, Division of Nephrology, Medical Clinic and Polyclinic IV, University of Munich, Schillerstr. 42, D-80336 Munich, Germany. Email: maciej.lech@med.uni-muenchen.de

accumulating experimental evidence that the associated immune response is an important determinant of AKI outcomes.[11] During the injury phase, necrotic tubules release molecules (*e.g.*, histones or high-mobility group protein B1) that activate Toll-like receptors (TLRs) and inflammasomes on interstitial mononuclear phagocytes to trigger the secretion of proinflammatory cytokines and chemokines.[12–17] Chemokines guide neutrophils and proinflammatory (M1 or classically activated) macrophages to enter the site of injury,[18] which largely account for the extent of tubular necrosis and thereby determine the extent of AKI.[19] The rapid apoptosis of the neutrophils changes the local microenvironment and phagocytic uptake of apoptotic neutrophils induces a functional switch of the macrophages toward an anti-inflammatory (M2 or alternatively activated) phenotype.[19,20] This macrophage phenotype not only supports the resolution of postischemic renal inflammation but also actively promotes healing (*i.e.*, tubular repair).[21–23] In fact, regenerative tubular epithelial cell proliferation starts as early as 3 hours after tubular injury; however, the resolution of renal inflammation seems to be mandatory to shift the balance of tubular repair and ongoing injury toward structural and functional tubular recovery,[24–26] similar to wound healing in general.[27] Therefore, factors that regulate macrophage phenotypes might determine AKI recovery and long-term outcomes.[21,28]

The IL-1 receptor–associated kinases (IRAKs) are important regulators of macrophage phenotype polarization because they are involved in the IL-1R/TLR/Myd88–dependent activation of NF-κB.[29] IRAK-4–mediated TNF receptor–associated factor 6 phosphorylation is an essential step of this signaling pathway,[30] which is inhibited selectively in monocytes and macrophages by IRAK-M.[31] This way, the delayed induction of IRAK-M deactivates classically activated macrophages, which contributes to endotoxin tolerance *in vitro*, resolution of inflammation *in vivo*, compensatory anti-inflammatory response syndrome during advanced sepsis, and immunosuppressive tumor environments, as well as limits autoimmune tissue injury.[31–39] IRAK-M–mediated deactivation of proinflammatory macrophages also limits immunopathology during infections as well as osteoclast-driven osteoporosis.[36,40]

We speculated that IRAK-M–mediated deactivation of proinflammatory mononuclear phagocytes is required for the resolution of renal inflammation to allow structural and functional tubular reconstitution as a determinant of long-term outcomes upon AKI. We used IRAK-M–deficient mice and long-term follow-up upon postischemic AKI to address this concept.

RESULTS

IRAK-M Expression Increases in the Postischemic Kidney but Does Not Contribute to Early AKI

We first studied IRAK-M mRNA expression in solid organs of healthy adult female C57BL/6 mice, which revealed high IRAK-M baseline expression in the kidney among other organs such as the urinary bladder, heart, muscle, skin, and spleen (Figure 1A). We next determined whether IRAK-M is present in immune or nonimmune cells in the kidney of healthy adult mice. IRAK-M mRNA was absent in nonactivated cells; however, LPS stimulation induced IRAK-M only in $CD11b^+$ myeloid cells as well as in a murine macrophage cell line (J774) (Figure 1B). To determine whether oxidative stress is another trigger for IRAK-M expression, we exposed primary mouse kidney $CD11b^+$ myeloid cells to the reactive oxygen species donor hypoxanthine/xanthine oxidase. A rapid increase in heat shock protein 70 expression, which served as a positive control for oxidative cell stress, was observed, whereas IRAK-M mRNA levels increased somewhat only after 24 hours (Figure 1C). To determine the role of IRAK-M in the acute phase of kidney injury, groups of sex-matched IRAK-$M^{-/-}$ and IRAK-$M^{+/+}$ mice underwent unilateral clamping of the renal pedicle for 45 minutes before kidneys were harvested at 1, 5, and 10 days after surgery. Surgery did not induce IRAK-M mRNA levels in sham kidneys, whereas they were significantly elevated at all time points in the postischemic kidney (Figure 1D). Renal cell suspensions taken at day 1 revealed that the induction of IRAK-M mRNA expression originated selectively from $CD11b^+$ immune cells and not from $CD11b^-$ renal parenchymal cells (Figure 1E). Postoperative injection of antioxidants suppressed heat shock protein 70 but not IRAK-M mRNA (Figure 1E), excluding oxidative stress as a direct trigger for IRAK-M induction. Importantly, lack of IRAK-M did not affect AKI upon bilateral renal artery clamping as evidenced by serum creatinine and urea, proinflammatory cytokine expression, tubular injury scores, and intrarenal neutrophil and macrophage accumulation at 24 hours (Supplemental Figure 1). Baseline serum creatinine levels did not differ between wild-type and IRAK-M–deficient mice (data not shown). Thus, IRAK-M is specifically induced in renal immune cells of the postischemic kidney. This, however, did not affect renal inflammation, immunopathology, and renal dysfunction during postischemic AKI.

Up to 45 Minutes of Unilateral Renal Pedicle Clamping Allows Full AKI Recovery

The lack of phenotype of IRAK-$M^{-/-}$ mice in early AKI allowed us to study the role of IRAK-M in renal regeneration versus progression to CKD. First we searched to identify an ischemia time that still allows full AKI recovery. Although unilateral kidney ischemia times of 90 or 120 minutes resulted in kidney atrophy and compensatory hypertrophy of the contralateral kidney 5 weeks later, renal sizes remained unchanged and kidney injury markers were absent (suggesting full structural recovery) 5 weeks after $\leq$45 minutes of ischemia (Supplemental Figure 2). Shrunken kidneys upon 90 or 120 minutes of ischemia displayed severe tubular atrophy and interstitial fibrosis (not shown), consistent with increased renal mRNA expression levels of the tubular injury marker neutrophil gelatinase-associated lipocalin, the proinflammatory and

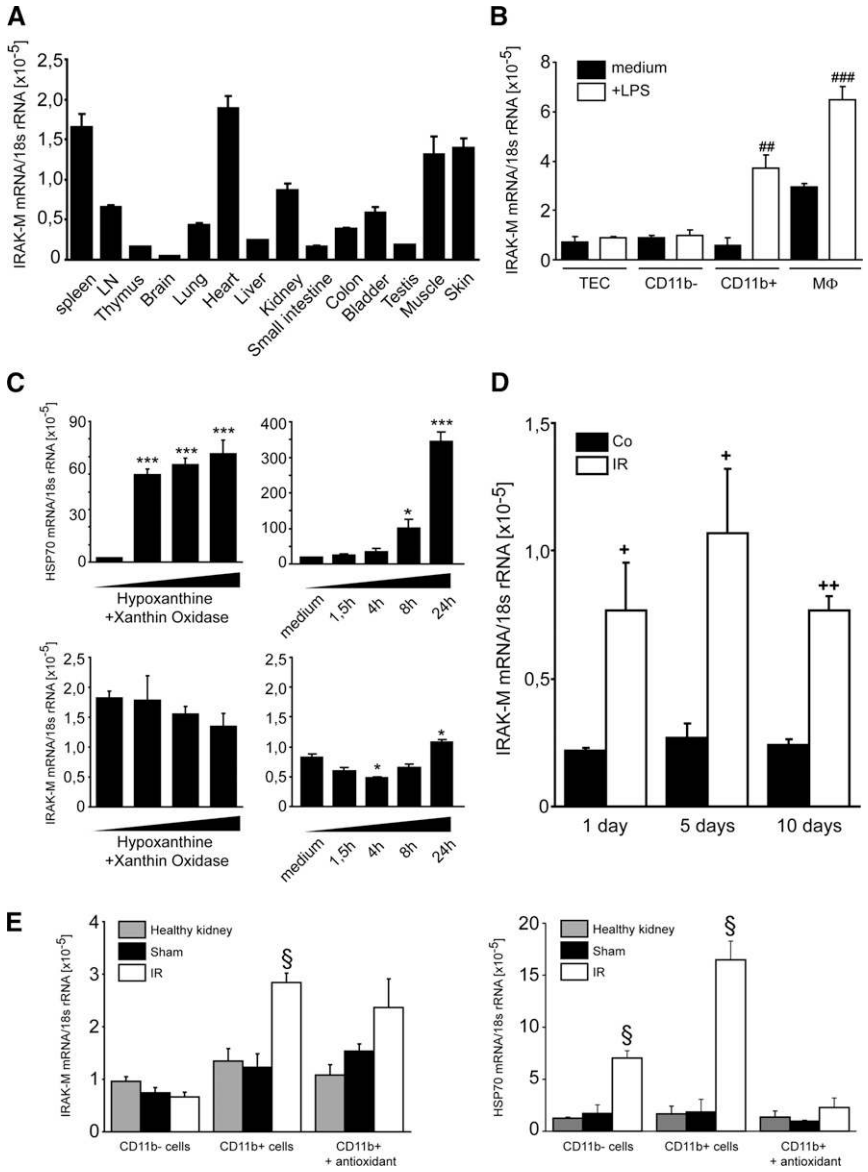

Figure 1. IRAK-M in AKI. IRAK-M mRNA expression is determined in organs from 10 mice (A) and renal cells from 5 mice (B) isolated by magnetic beads from 6-week-old female C57BL/6 mice or a macrophage cell line (MΦ), respectively. $^{\#\#}P<0.01$; $^{\#\#\#}P<0.001$. (C) IRAK-M CD11b$^+$ myeloid cells are exposed to 2.5 mM of hypoxanthine and 0.005 of U/ml xanthine oxidase, and HSP70 and IRAK-M mRNA expression are determined after different time points as indicated. Data are mean ratios of the specific mRNA and the respective 18s rRNA level ± SEM from three independent experiments. $^*P<0.05$; $^{***}P<0.001$ versus time point zero. (D) IRAK-M mRNA levels are determined by RT-PCR in postischemic or sham-operated kidneys at 1, 5, or 10 days after unilateral renal pedicle clamping of sex-matched mice. Data are mean ratios of the specific mRNA and the respective 18s rRNA level ± SEM from three independent experiments. $^+P<0.05$; $^{++}P<0.01$; versus sham control of the same time point. (E) Renal CD11b$^+$ and CD11b$^-$ cells are isolated 1 day after unilateral renal pedicle clamping of mice injected with either PBS or antioxidant. IRAK-M and HSP70 mRNA expression levels are determined by real-time RT-PCR. Data are expressed as mean of the ratio versus the respective 18s rRNA level ± SEM. $^{\S}P<0.05$ versus wild-type kidneys of the same time point. LN, lymph node; HSP70, heat shock protein 70.

proapoptotic cytokine TNF-α, and the profibrotic mediators TGF-β and connective tissue growth factor (Supplemental Figure 2). Because all of these parameters remained unaffected 5 weeks after AKI, we used 45 minutes of ischemia time in all further experiments.

Lack of IRAK-M Leads to Tubular Atrophy Instead of Tubular Repair upon AKI

We speculated that IRAK-M would have a functional role, if not in the early phase of AKI, then during subsequent healing and recovery. In fact, the maximum of intrarenal IRAK-M induction was found 3 weeks after 45 minutes of unilateral renal pedicle clamping (Figure 2A). In contrast to full AKI recovery of wild-type mice, kidneys of IRAK-M–deficient mice displayed a progressive loss of kidney weight, mirrored by compensatory hypertrophy of the contralateral kidney as determined 3, 5, 7, and 10 weeks after AKI (Figure 2, B and C). This largely resulted from a loss of tubules as evidenced by staining and digital morphometry for *Lotus tetragonobulus* lectin after 5 weeks, especially when referred to the remaining kidney mass (Figure 2, D and E). This was consistent with significantly reduced E-cadherin mRNA expression levels at 3, 5, and 10 weeks after postischemic AKI (Figure 3A). A significant reduction of bromodeoxyuridine-positive/E-cadherin–positive tubular epithelial cells (TECs) suggested a lack of regenerative epithelial cell proliferation as one causal element of tubular atrophy at 5 weeks (Figure 3B). Another morphologic hallmark of atrophic kidneys in IRAK-M$^{-/-}$ mice was the increased cortical density of glomeruli at 5 weeks (Figure 3C), which were confirmed to largely represent atubular glomeruli on serial sections stained with *L. tetragonobulus* lectin to identify the anatomy of the glomerular-tubular junction (Figure 3D). This was further confirmed by microdissecting nephrons from IRAK-M–deficient atrophic kidneys, which displayed all stages of degeneration of the glomerular-tubular junction (Figure 3E). IRAK-M is needed to prevent progressive tubular atrophy and the formation of atubular glomeruli in the recovery phase of postischemic AKI.

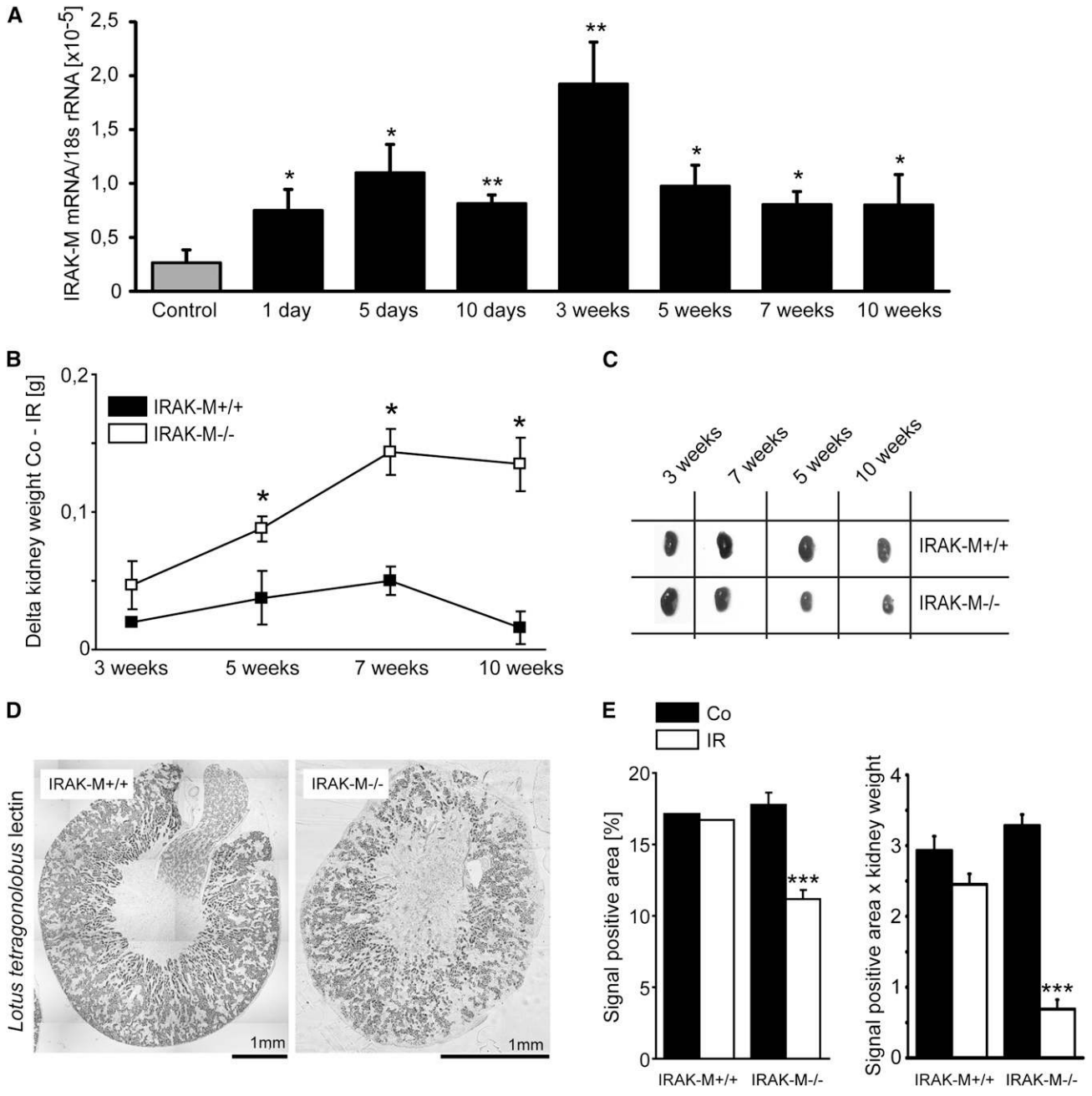

Figure 2. Lack of IRAK-M and postischemic tubular loss. (A) IRAK-M mRNA levels are determined by RT-PCR in postischemic or sham-operated kidneys at 1, 5, and 10 days and 3, 5, 7, or 10 weeks after renal pedicle clamping. Data are mean ratios of the specific mRNA and the respective 18s rRNA level ± SEM. (B) Mean Δ kidney weight (contralateral minus postischemic kidney) ± SEM from at least five mice upon 45 minutes of ischemia time analyzed at the indicated time points. *$P<0.05$ versus wild-type mice of the same time point. Note that for IRAK-M$^{-/-}$ mice, the weight difference between the contralateral and postischemic kidney is significantly larger at 5, 7, and 10 weeks, indicating more loss of kidney mass in the ischemic kidney and more hypertrophy of the contralateral kidney, respectively. (C) Representative postischemic (IR) and control kidneys from both mouse strains are shown to illustrate kidney atrophy versus compensatory hypertrophy. (D) Kidneys after 45-minute IRI at 5 weeks after surgery are stained with *L. tetragonolobus* lectin to identify proximal tubules (note the different size of the scale bar, implying the much smaller size of the IRAK-M$^{-/-}$ kidney). (E) Quantitative analysis of *L. tetragonolobus* lectin staining expressed either in percentage of positive area or relative to kidney weight. ***$P<0.001$ versus wild-type mice.

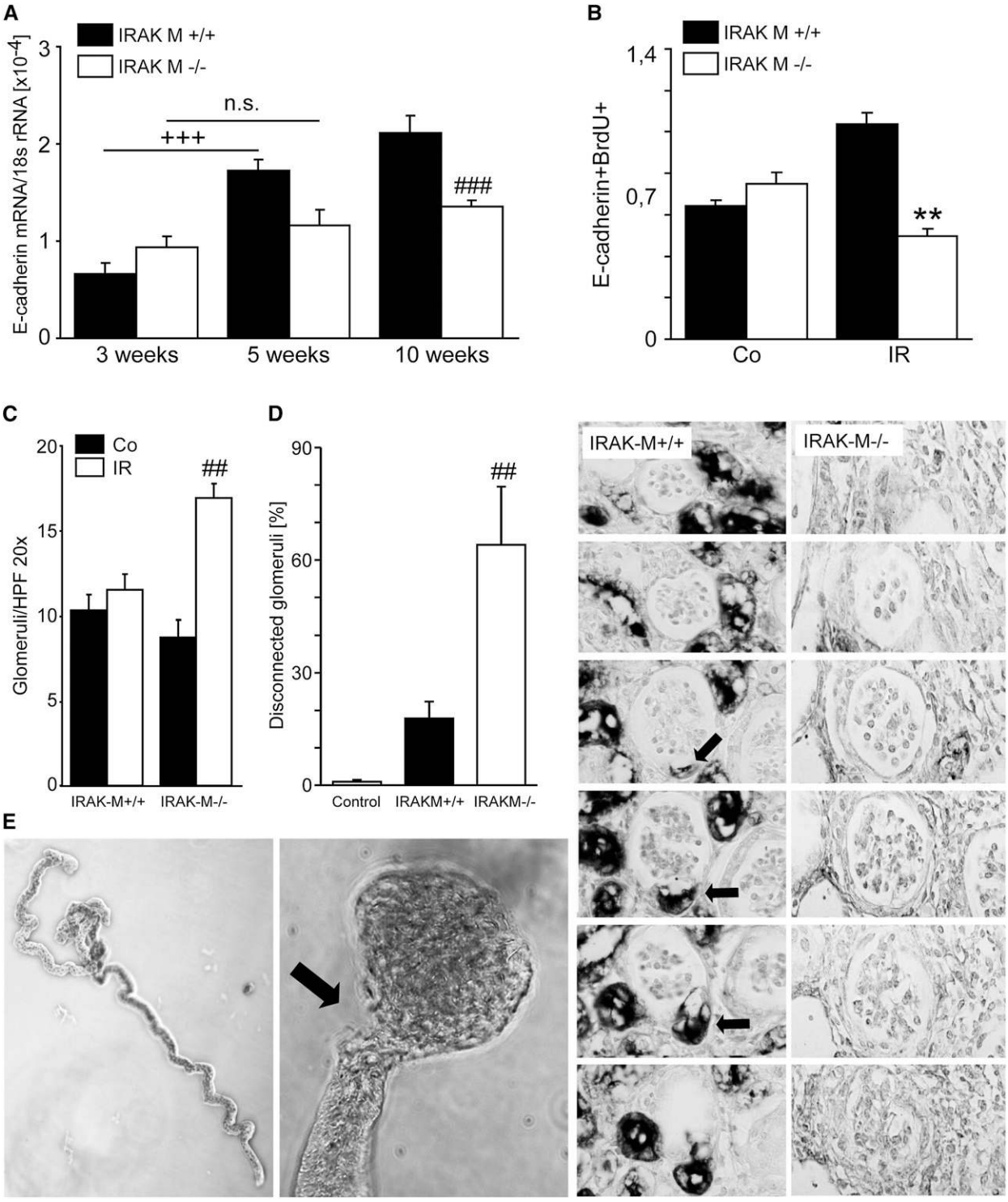

Figure 3. Lack of IRAK-M and postischemic tubular loss. (A) Numbers of tubular cells are estimated by quantitative PCR for E-cadherin at 3, 5, and 10 weeks postsurgery. $^{+++}P<0.001$; $^{\#\#\#}P<0.001$. (B) Proliferating tubular cells are quantified by flow cytometry for E-cadherin and BrdU at 5 weeks as described in Concise Methods. Data are mean ratios ± SEM. $^{**}P<0.01$ versus control (Co) kidney or ischemic (IR) kidney from wild-type mice. (C) At 5 weeks, the cortical density of glomeruli is determined in IR and Co kidneys as described in Concise Methods. Data are mean ratios ± SEM. $^{\#\#}P<0.01$ versus ischemic kidney from wild-type mice. (D) At 5 weeks, atubular glomeruli are identified in ischemic kidney using *L. tetragonolobus* lectin staining. The glomerulotubular junction is indicated by arrows. (E) Nephron microdissection reveals mostly intact nephrons from control kidneys (upper image) and nephrons with partially or complete disconnection at the glomerular-tubular junction (arrow) IR kidneys of IRAK-M–deficient mice. BrdU, bromodeoxyuridine; HPF, high-power field; n.s., not significant. Original magnification, ×200.

Tubular Atrophy in IRAK-M$^{-/-}$ Mice Is Associated with Interstitial Fibrosis

CKD upon AKI is usually characterized not only by tubular atrophy but also by interstitial fibrosis (*i.e.,* progressive accumulation of extracellular matrix produced mostly by interstitial myofibroblasts).[41,42] We quantified this process by smooth muscle actin and Masson trichrome staining. Lack of IRAK-M was associated with a significant increase in interstitial fibrosis 5 weeks after renal pedicle clamping (Figure 4A). This was consistent with increased mRNA expression levels of fibrosis markers such as laminin, fibronectin, collagen I, collagen IVα1, and fibroblast-specific protein 1 (FSP-1) in postischemic kidneys of IRAK-deficient mice compared with kidneys from wild-type control mice (Figure 4B). In addition, we determined the mRNA expression levels of the profibrotic factors TGF-β and connective tissue growth factor, proinflammatory TNF-α, and the tubular injury marker neutrophil gelatinase-associated lipocalin at three different time points. Their expression levels all progressively increased over time in IRAK-M–deficient versus wild-type postischemic kidneys (Figure 4C). IRAK-M is needed to prevent not only tubular atrophy and atubular glomeruli formation during the recovery phase of postischemic AKI but also the associated progressive interstitial inflammation and fibrosis.

Lack of IRAK-M Is Associated with Persistent Proinflammatory Macrophage Infiltrates in the Postischemic Kidney

Because IRAK-M was selectively induced in mononuclear phagocytes of the postischemic kidney, we carefully characterized these cells in kidneys of both genotypes by F4/80 immunostaining and flow cytometry. F4/80$^+$ macrophage infiltrates were almost absent in wild-type kidneys 5 weeks after renal pedicle clamping. In contrast, these cells were massively increased in the renal interstitial compartment of IRAK-M$^{-/-}$ mice starting from 3 weeks after renal pedicle clamping (Figure 5A and Supplemental Figure 3). This was consistent with increased renal mRNA expression levels of proinflammatory cytokines/chemokines such as TNF-α, chemokine (C-C motif) ligand 2, and C-X-C motif chemokine 10 (Figure 5B), all known to be released by activated proinflammatory macrophages.[43] To confirm this, we performed quantitative flow cytometry of renal cell suspensions from kidneys of both genotypes 5 weeks after renal pedicle clamping. IRAK-M–deficient mice showed a significantly increased number of CD45$^+$ and CD11b$^+$ cells (Figure 5C). To test for their activation state, we quantified Ly6C^h-positive or TNF-α–positive CD11b cells because these populations mostly represent the classically activated proinflammatory mononuclear phagocyte phenotype. IRAK-M–deficient mice displayed significantly increased numbers of intrarenal Ly6C^{hi}-positive cells compared with wild-type control kidneys (Figure 5C). This was consistent with increased mRNA expression levels of M1-dependent genes at 3 weeks (Figure 5D). For example, M1 marker inducible nitric oxide synthase (but not M2 marker Arg1) was increased starting from 3 weeks after pedicle clamping (Supplemental Figure 3), which was consistent with the aforementioned increase in renal macrophage infiltrates. Furthermore, IRAK-M–deficient macrophages produced significantly higher amounts of TNF-α and lower amounts of IL-10 upon stimulation with LPS (Figure 5E). In addition, coculture experiments demonstrated that IRAK-M–deficient macrophages have a higher potential to kill tubular cells, whereas the tubular cell genotype does not affect these results (Supplemental Figure 4). The effect of IRAK-M deficiency on chronic AKI outcome could also be mimicked by injections of the TLR9 ligand CpG DNA, which specifically activates macrophages toward the M1 phenotype[44] (Supplemental Figure 5). In IRAK-M–deficient mice, AKI is followed by tubular atrophy in association with a persistent intrarenal accumulation of classically activated mononuclear phagocytes that express proinflammatory and proapoptotic mediators, including TNF-α. A similar effect is seen upon injection of a TLR9 agonist, known to activate renal macrophages *in vivo* toward an M1 phenotype.

TNF-α Blockade Partially Prevents CKD upon AKI in IRAK-M–Deficient Mice

The CKD phenotype of IRAK-M–deficient mice was linked to activated mononuclear phagocytes that produce TNF-α. Therefore, we wanted to validate their functional relevance for this phenotype by an interventional approach (*e.g.,* by blocking TNF-α). We treated IRAK-M–deficient mice with the TNF-α antagonist etanercept every alternate day, starting from day 5 (Figure 6A). Etanercept significantly prevented loss of kidney mass of the postischemic kidney and the compensatory hypertrophy of the contralateral kidney (Figure 6B). Moreover, it reduced the amount of intrarenal F4/80$^+$ macrophages (Figure 6C). This was associated with a significant protection from tubular atrophy (as evidenced by morphometry of the *L. tetragonobulus* lectin–positive area) and from renal fibrosis (as quantified by Masson trichrome staining) (Figure 6C).

Upon AKI, intrarenal mononuclear phagocytes need IRAK-M to suppress their persistent polarization into a proinflammatory phenotype. This way, IRAK-M prevents intrarenal secretion of proinflammatory and proapoptotic cytokines such as TNF-α, which promote subsequent tubular atrophy (*i.e.,* CKD instead of full recovery from AKI).

DISCUSSION

We speculated that IRAK-M–mediated suppression of inflammatory mononuclear phagocytes would be required for the resolution of renal inflammation to allow full recovery of AKI. Our studies using IRAK-M–deficient mice confirm this concept and further demonstrate that the persistence of inflammatory renal mononuclear phagocytes is sufficient to compromise kidney regeneration and cause progressive CKD instead. These findings modify several of the current concepts about AKI and CKD. First, effective kidney regeneration requires the resolution

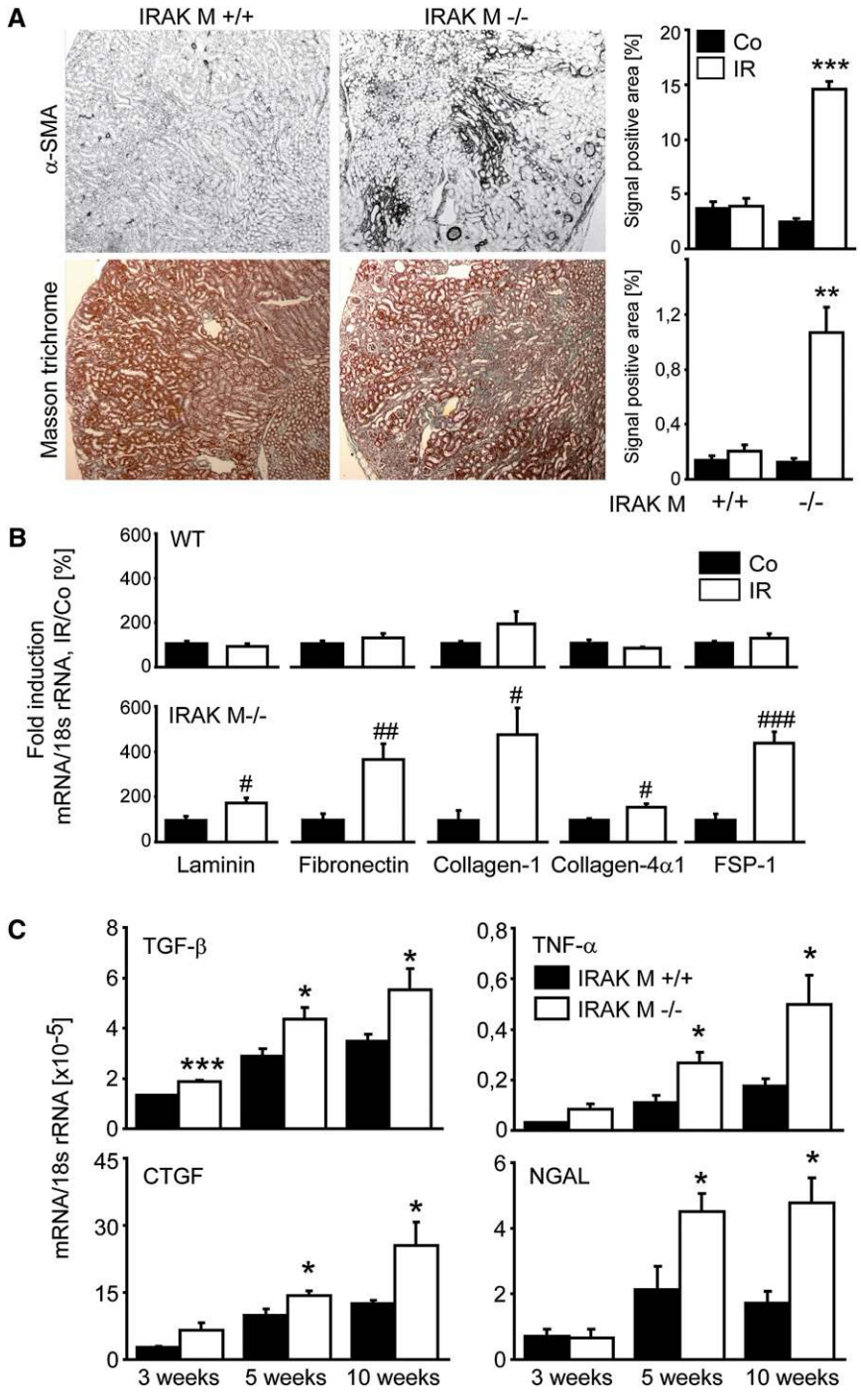

Figure 4. Lack of IRAK-M and kidney fibrosis. (A) Renal tissue is obtained at 5 weeks after unilateral renal pedicle clamping and stained for markers of fibrosis (*e.g.*, α-SMA). Representative images are shown for both genotypes. The quantitative analyses are performed using image software as described in Concise Methods and are expressed as means ± SEM of positivity per high-power field. $^{**}P<0.01$; $^{***}P<0.001$ versus wild-type mice of the same time point. (B and C) Total RNA is extracted from ischemic (IR, white bars) and contralateral (Co, black bars) kidneys of IRAK-M–deficient or wild-type mice at 5 weeks (B) and at different time points (C); mRNA expression levels are determined for the indicated targets by real-time RT-PCR. Data are expressed as mean of the ratio versus the respective 18s rRNA level ± SEM. $^{\#}P<0.05$; $^{\#\#}P<0.01$; $^{\#\#\#}P<0.001$ versus contralateral kidneys (B); and $^{*}P<0.05$ versus wild-type kidneys of the same time point (C), respectively. α-SMA, α-smooth muscle actin; WT, wild-type; FSP-1, fibroblast-specific protein 1; CTFG, connective tissue growth factor; NGAL, neutrophil gelatinase-associated lipocalin. Original magnification, ×50.

of inflammation. Second, resolving renal inflammation is an active, not passive, process that depends on the induction of genes like IRAK-M that deactivate proinflammatory mononuclear phagocytes. Third, our data argue against the role of alternatively activated (M2) macrophage-mediated renal fibrosis to cause CKD. CKD rather results first from persistent inflammation-driven tubular atrophy. Fourth, kidney shrinkage in CKD upon AKI resulted predominately from the loss of tubules, not from the loss of glomeruli or from excessive interstitial fibrosis. This observation is in line with several other recently published studies that altogether question the dogma of (M2 macrophage-driven) renal fibrosis being a cause of CKD.[24,45,46] Fifth, a single macrophage gene defect was sufficient to turn full AKI recovery into progressive CKD, which implicates that genetic factors determine long-term outcomes of AKI. Sixth, this is the first report to document a role of IRAK-M in wound healing or tissue regeneration. Finally, transient CpG DNA exposure, a synthetic mimic of bacterial DNA, had the same effect, suggesting that environmental factors like infections can affect long-term outcomes of AKI.

IRAK-M is an intracellular signaling molecule that suppresses the nonredundant proinflammatory effects of other IRAKs of the IL-1R/TLR signaling cascade.[31] IRAK-M–deficient mice display several characteristics that relate to a shift toward the classically activated proinflammatory mononuclear phagocyte phenotype, including the lack of endotoxin tolerance or the development of activated osteoclast-related osteoporosis, respectively.[36,38] Upon TLR activation, IRAK-M expression is induced with some delay to the proinflammatory mediators for the subsequent inhibition of the inflammatory response.[38] This mononuclear phagocyte deactivation is an essential element of the phenomenon of endotoxin tolerance *in vitro* as well as the compensatory anti-inflammatory response

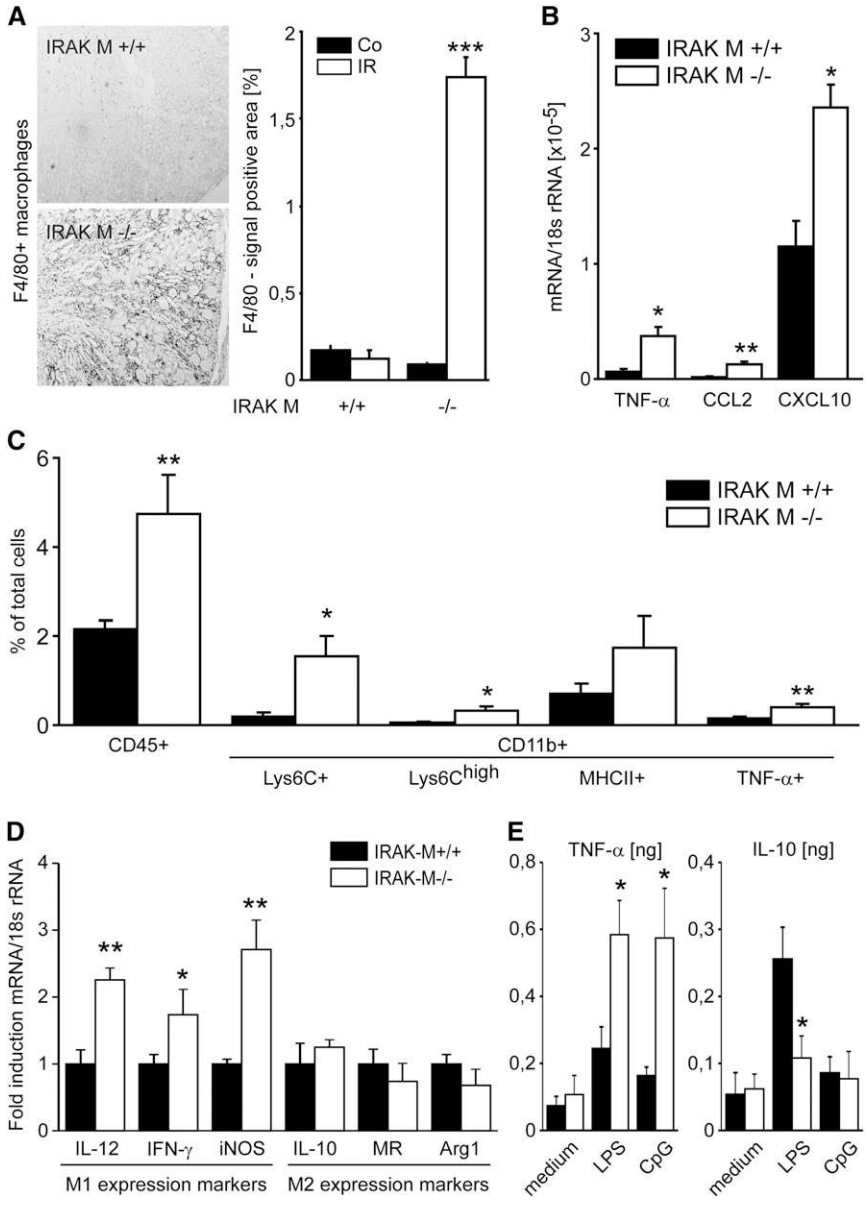

Figure 5. Lack of IRAK-M and macrophage recruitment to postischemic kidneys. (A) Renal tissue is obtained at 5 weeks after unilateral renal pedicle clamping and stained for F4/80$^+$ renal mononuclear phagocytes. Representative images are shown for both genotypes and each time point. The quantitative analyses are performed using image software as described in Concise Methods and are expressed as means ± SEM of positivity per high-power field. ***P<0.001 versus wild-type mice of the same time point. (B) Total RNA is extracted from leukocytes of ischemic kidney from IRAK-M–deficient (white bars) or wild-type mice (black bars). Specific macrophage markers are investigated by quantitative PCR. All data are presented as means ± SEM. *P<0.05; **P<0.01; ***P<0.005. (C) Characterization of macrophages by flow cytometry shows increased mRNA levels of M1 but not M2 markers in IRAK-M–deficient mice at 3 weeks. All data are presented as means ± SEM. *P<0.05; **P<0.01 versus IR kidneys of wild-type mice. (D) Characterization of macrophages by mRNA expression shows increased mRNA levels of M1 but not M2 markers in IRAK-M–deficient mice at 3 weeks. All data are presented as means ± SEM. *P<0.05; **P<0.01 versus IR kidneys of wild-type mice. (E) CD11b$^+$ cells are stimulated *in vitro* with TLR ligands. Supernatants are analyzed for TNF-α and IL-10 by ELISA. iNOS, inducible nitric oxide synthase. Original magnification, ×50.

syndrome during human sepsis.[38] The same resolution of inflammation is also needed in transient sterile injuries to allow tissue recovery by (epithelial) regeneration. We previously showed that single Ig and Toll-IL-1 receptor and IFN regulatory factor 4 IRF4, two other negative regulators of IL-1R/TLR signaling, limit the early injury phase of postischemic AKI[47–49]; however, these factors are expressed predominately by renal dendritic cells that orchestrate the early injury phase of AKI.[19] In contrast, IRAK-M is predominately expressed by macrophages that recruit to the kidney only later and significantly contribute to the healing phase of AKI.[19,21,22] In the healing phase, anti-inflammatory macrophages predominate because they are needed to remove cell debris and to enforce the resolution of inflammation as well as epithelial regeneration.[20,21] Lack of IRAK-M seems to maintain a proinflammatory mononuclear phagocyte phenotype, which is obviously sufficient to compromise epithelial repair, a phenomenon previously demonstrated in skin wounding.[27,50] Lack of rapid epithelial regeneration subsequently activates mesenchymal healing (*i.e.*, fibrosis),[24] which results in defective repair but no longer in regeneration, a common characteristic of tissue remodeling in CKD.[9,41,42,51,52]

Since Mantovani *et al.* introduced macrophage polarization based on *in vitro* studies in 2004,[43] renal scientists have favored the concept that proinflammatory and regulatory macrophages both contribute to poor outcomes in kidney disease.[52] Although the role of inflammatory macrophages for immunopathology in AKI and CKD was clear, the role of other macrophage phenotypes was less certain. Alternatively activated macrophages produce anti-inflammatory as well as profibrotic factors, which help the resolution of inflammation but also promote tissue fibrosis. We prefer the view of the tissue's attempt to regain homeostasis upon injury and that the tissue recruits macrophages to support either regeneration or repair to regain homeostasis as well as possible.[51,53] As such, immunoregulatory macrophages have an important role in resolving inflammation and supporting regeneration[21] or, if not possible, at least repair, which implies mesenchymal healing to stabilize the tissue.

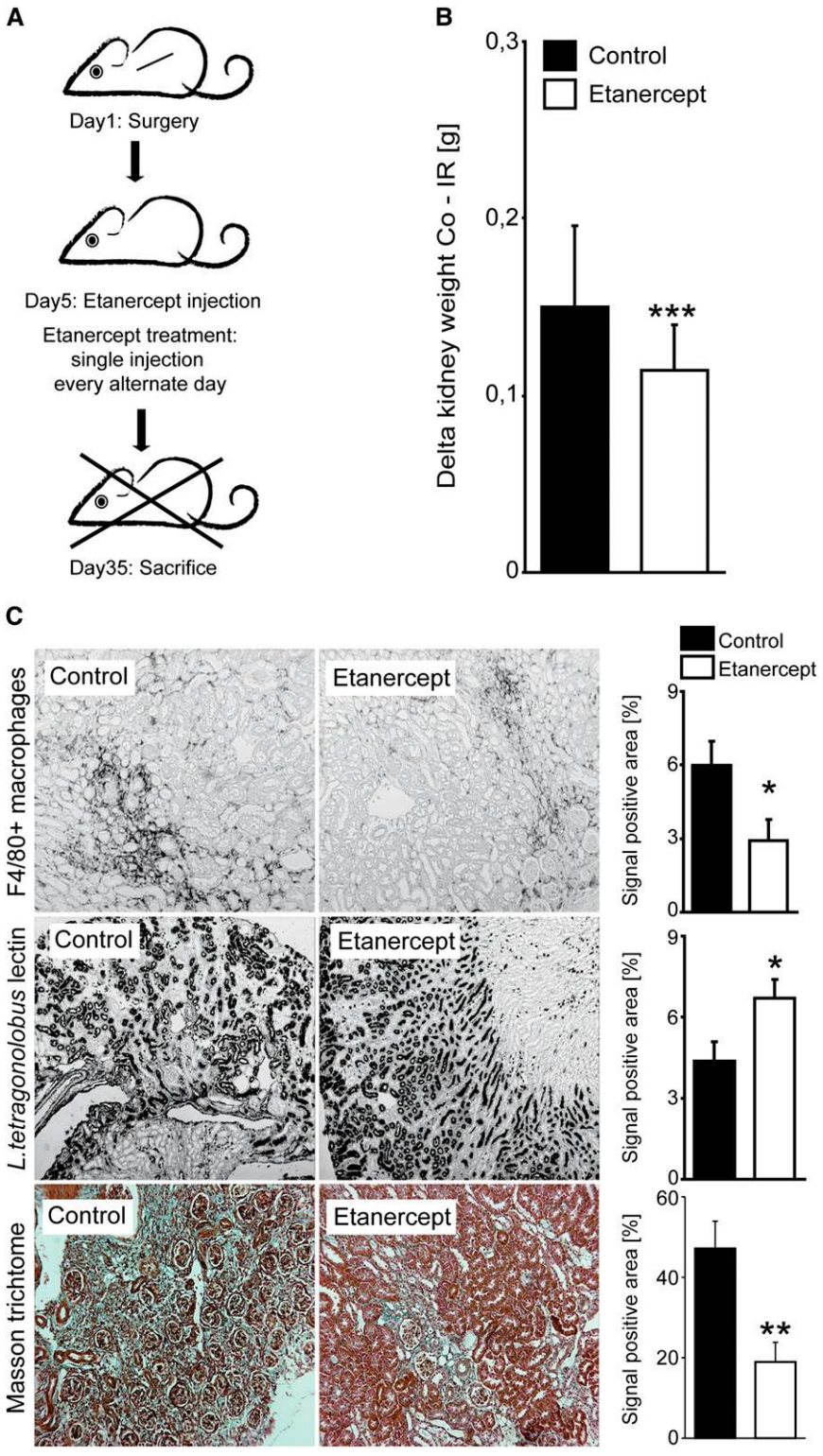

Figure 6. Treatment of postischemic AKI with etanercept. (A) IRAK-M mice undergo unilateral renal pedicle clamping as described in Concise Methods. Groups of mice (n=15) receive vehicle control or 10 mg/kg etanercept intraperitoneally given on every alternate day starting 5 days after reperfusion. (B) Loss of weight of ischemic kidney (IR) is compared with contralateral kidney (Co) from both treated and control IRAK-M mice. Data are presented as means ± SEM. ***P<0.001. (C) Renal tissue is obtained at 5 weeks after unilateral renal pedicle clamping and stained with *L. tetragonolobus* lectin or Masson trichrome. Representative images are shown for both genotypes and each time point. The quantitative analyses are performed using image software as described in Concise Methods and are expressed as means ± SEM of positivity per high-power field; *P<0.05 versus wild-type mice of the same time point. Original magnification, ×50.

Here we show that lack of IRAK-M or bacterial DNA exposure leads to persistence of inflammatory mononuclear phagocytes that promote persistent inflammation, subsequent tubular atrophy, and scarring, which display macroscopically as shrunken kidneys. This, in turn, implies that immunoregulatory macrophages are needed for recovery, and their association with renal fibrosis rather indicates their insufficient capacity to always promote sufficient epithelial repair, a concept supported by studies from several other groups.[20–22,45,46,54]

We conclude that IRAK-M deficiency is sufficient to turn AKI recovery into progressive CKD, because IRAK-M is needed to suppress persistent macrophage-related renal inflammation. This implies the following: (*1*) kidney regeneration first requires the resolution of renal inflammation; (*2*) resolution of kidney inflammation is an active, not passive, process; (*3*) alternatively activated mononuclear phagocytes support epithelial regeneration; (*4*) kidney shrinkage in CKD upon AKI mostly results from the loss of tubules; (*5*) genetic and environmental factors can negatively affect long-term outcomes of AKI by modulating renal mononuclear phagocyte activation state; and (*6*) IRAK-M contributes to tissue regeneration.

CONCISE METHODS

Animal Studies

IRAK-M–deficient mice were generated and backcrossed to the C57BL/6 strain (B6; Charles River Laboratories, Calco, Italy) to the F9 generation. Mice were housed in groups of five in filter top cages with unlimited access to food and water. Cages, nestlets, food, and water were sterilized by autoclaving before use. Groups of age- and sex-matched littermate mice (n=6–9) were

anesthetized before renal pedicle clamping (unilateral, 45 minutes; bilateral, 30 minutes or 45 minutes) with a microaneurysm clamp *via* flank incisions (Medicon, Tuttlingen, Germany) as previously described.[55] Body temperature was maintained at 37°C throughout the procedure by placing the mice on a heating pad. After clamp removal, the kidney was inspected for restoration of blood flow evidenced by returning to its original color before closing the wound with standard sutures. To maintain fluid balance, all mice were supplemented with 1 ml of saline administered subcutaneously. The contralateral kidney was left untouched and used as a control (see Figure 1). For sham surgeries, the mice were kept under anesthesia and kidneys were examined without clamping the pedicles. Mice were euthanized 1, 5, 10, 15, 21, 35, 49, and 70 days after renal pedicle clamping and both kidneys were weighed and divided to be either snap frozen in liquid nitrogen, frozen in RNAlater, or fixed in 10% buffered formalin. For histologic assessment of renal fibrosis, immune cells infiltration and glomerular density slides were examined under a microscope and quantified by counting colorimetric areas using Adobe Photoshop software (Adobe, San Jose, CA) as previously described.[56] Groups of IRAK-M$^{-/-}$ and wild-type mice (n=7–15 per group) were unilaterally operated and maintained for 5 weeks before euthanasia. In further experiments, IRAK-M–deficient mice were injected intraperitoneally with 10 mg/kg of etanercept every second day starting from day 5. At age 4 weeks, groups of wild-type mice (n=8) began receiving 14 intraperitoneal injections of 100 μl of PBS or 40 μg of endotoxin-free CpG-phosphothioate oligonucleotide 1668 (5′-TCGATGACGTTCCTGATGCT-3′; TIB-Molbiol, Berlin, Germany) on alternate days starting from day 5. The cohorts were euthanized 35 days after ischemic injury. All experiments were performed according to the Guide for the Care and Use of Laboratory Animals and were approved by a governmental review board. BUN and serum creatinine levels were measured using a commercially available kit (DiaSys Diagnostic Systems, Holzheim, Germany).

Renal Cell Isolation

Kidneys were mechanically disrupted and incubated in 1× Hanks' balanced salt solution containing 1 mg/ml of collagenase type I and 0.1 mg/ml of deoxyribonuclease type I (Sigma-Aldrich, Steinheim, Germany) for 20 minutes at 37°C. After washes, tissues were incubated in 5 ml of 2 mM EDTA in Hanks' balanced salt solution (without calcium and magnesium) for 20 minutes at 37°C. The supernatant containing isolated cells was kept on ice; for a second enzyme step, the remaining pellet was incubated in 5 ml of 1 mg/ml collagenase I in Hanks' balanced salt solution for 20 minutes at 37°C. The suspension was subsequently passed through 19- and 27-gauge needles, and pooled with the first supernatant from the EDTA incubation. Cells were filtered through a 70-μm cell strainer (BD Biosciences, Heidelberg, Germany) and washed twice in PBS. All washing steps were performed in FACS buffer (PBS containing 0.2% of BSA and 0.1% of NaAzide). Renal leukocytes were characterized by using flow cytometry using a FACSCalibur machine (BD Biosciences). For some studies, renal CD11b^{+} macrophages were isolated from renal cell suspensions by using microbead-conjugated antibodies (Miltenyi Biotech, Bergisch-Gladbach, Germany). Magnetic bead separation was done according to the manufacturer's instructions. M1/M2 expression pattern mRNA levels were determined by quantitative RT-PCR. Primary TECs were isolated from 6-week-old C57BL/6 wild-type mice. Kidney-cell suspensions were prepared by applying the mashed kidney onto 30-μm preseparation filters (Miltenyi Biotec). The cell suspension was incubated for 2 hours at 37°C and the nonadherent cells were harvested and applied to culture dishes coated with collagen I (Sigma-Aldrich, Taufkirchen, Germany) in predefined K1 medium. Mouse TECs were seeded (5×105 cells/ml) in 10% FCS 1% 50,000 cells/ml DMEM medium on six-well plates and grown overnight to subconfluence. Purity was characterized by immunostaining with TEC surface markers E-cadherin and cytokeratin-7, and was determined to be >90%. For spleen monocytes, spleen single-cell suspension was prepared in Roswell Park Memorial Institute (RPMI) medium by passage through a 70-μm cell strainer. For purification of splenocytes, cells were centrifuged at 1800×g for 5 minutes at 4°C. The pelleted cells were collected and flushed through a 30-μm filter. For further purification, the cell fraction was washed with RPMI, suspended into 0.155 M NH_4CL and incubated for 15 minutes to lyse erythrocytes. Cells were washed twice, centrifuged, and suspended in the same medium at 1×10^7 cells/ml, and plated into a six-well plate. The plate was incubated at 37°C for 45 minutes in a 5% CO_2 incubator. Nonadherent cells were then collected using warm RPMI (37°C). This step was repeated twice. Cells were treated with 2.5 mmol/L of hypoxanthine (Sigma-Aldrich) and 0.005 U/ml of xanthine oxidase (Sigma-Aldrich) serving as reactive oxygen species donors. Levels of mRNA were determined by quantitative RT-PCR. Bone marrow dendritic cells were prepared from wild-type mice and maintained in an RPMI conditioning medium containing 1 μg/ml of GM-CSF for 7 days in order to enrich the amount of myeloid cells. Ultrapure LPS (1 μg/ml) or CpG DNA (1 μg/ml) were used to stimulate 5×10^6 cells in 12-well plates. TNF and IL-10 ELISAs were performed according to the manufacturers' protocols (OptEiA; BD Biosciences).

Histologic Evaluation

Kidneys were embedded in paraffin and 2-μm sections for periodic acid–Schiff staining and immunostaining was performed as described. Postischemic tubular injury was scored by assessing the percentage of tubules in the corticomedullary junction that displayed cell necrosis, loss of the brush border, cast formation, and tubular dilation as follows: 0, none; 1, ≤10%; 2, 11%–25%; 3, 26%–45%; 4, 46%–75%; and 5, >76%. The following primary antibodies were used for immunostaining: rat anti-F4/80 (1:50; Serotec, Oxford, UK) for detection of macrophages, and rat anti-mouse Ly-6B.2 for detection of neutrophils (1:50; Serotec). To quantify interstitial cells, five corticomedullary high-power fields (×50) were digitally analyzed. Formalin-fixed tissues were stained with Masson trichrome and anti-smooth muscle actin antibodies, as well as *L. tetragonolobus* lectin for detection of fibrosis and loss of tubular compartments, respectively.

RNA Preparation and Real-Time Quantitative RT-PCR

RT and real-time RT-PCR from total renal RNA were prepared as previously described.[57] The SYBR Green dye detection system was used for quantitative real-time PCR on a Light Cycler 480 (Roche, Mannheim, Germany). Gene-specific primers (300 nM; Metabion, Martinsried, Germany) were used as listed in Table 1. Controls consisting of ddH2O were negative for target and housekeeper genes.

Table 1. Primers used for RT-PCR

Gene Name	Accession Number	Primer Sequences
IRAKM/IRAK3	NM_028679	Reverse: CCAGCCAGCTGTTTGAAAGT
		Forward: CACTGCTGGGAGAGCTTTG
Hsp70/Hspa1b	NM_010478	Reverse: ATGACCTCCTGGCACTTGTC
		Forward: GCTCGAGTCCTATGCCTTCA
TNF-α	NM_011609	Reverse: CCACCACGCTCTTCTGTCTAC
		Forward: AGGGTCTGGGCCATAGAACT
CCL2/MCP-1	NM_011333	Reverse: ATTGGGATCATCTTGCTGGT
		Forward: CCTGCTGTTCACAGTTGCC
TGF-β1	NM_011577	Reverse: CAACCCAGGTCCTTCCTAAA
		Forward: GGAGAGCCCTGGATACCAAC
CTGF	NM_010217	Reverse: CCGCAGAACTTAGCCCTGTA
		Forward: AGCTGACCTGGAGGAAAACA
NGAL/Lcn2	NM_008491	Reverse: ATTTCCCAGAGTGAACTG
		Forward: AATGTCACCTCCATCCTG
E-cadherin/Cdh1	NM_009864	Reverse: CCACTTTGAATCGGGAGTCT
		Forward: GAGGTCTACACCTTCCCGGT
Lamininβ2/Lamb2	NM_008483	Reverse: TCAGCTTGTAGGAGATGCCA
		Forward: CATGTGCTGCCTAAGGATGA
Fibronectin1/Fn1	NM_010233	Reverse: ACTGGATGGGGTGGGAAT
		Forward: GGAGTGGCACTGTCAACCTC
Collagen-1/Col1a1	NM_007742	Reverse: TAGGCCATTGTGTATGCAGC
		Forward: ACATGTTCAGCTTTGTGGACC
Collagen-4α1	NM_009931	Reverse: CACATTTTCCACAGCCAGAG
		Forward: GTCTGGCTTCTGCTGCTCTT
FSP-1/S100a4	NM_011311	Reverse: TTTGTGGAAGGTGGACACAA
		Forward: CAGCACTTCCTCTCTCTTGG
CXCL10	NM_021274	Reverse: ATGGATGGACAGCAGAGAGC
		Forward: GGCTGGTCACCTTTCAGAAG
18s	NR_003278	Reverse: AGGGCCTCACTAAACCATCC
		Forward: GCAATTATTCCCCATGAACG

Flow Cytometry

To determine the effects of renal injury on macrophage deposition and phenotype, kidneys were harvested at day 15 postinjury. Single-cell suspensions were prepared for flow cytometry as previously described.[44] After centrifugation (700×*g*, 20 minutes, without brake), the mononuclear cell population (>90% $CD45^+$) was removed carefully and washed with PBS. Cells were resuspended in 1 ml of PBS containing 0.5% of BSA and 0.2 μM of EDTA and incubated with antibodies against mouse CD45, Ly6c, TNF-α, and MHCII. All antibodies were obtained from BD Biosciences. Groups of mice were *in vivo*–labeled with bromodeoxyuridine according to the manufacturer protocol (BD Biosciences). Renal cells were stained for E-cadherin to assess the double-positive proliferating tubular cells. Cell numbers were counted and analyzed using flow cytometry (FACSCalibur; BD Biosciences). The total cell numbers and numbers of the different macrophage populations in every kidney were estimated using the counting beads.

Statistical Analyses

One-way ANOVA followed by a *post hoc* Bonferroni's test was used for multiple comparisons using GraphPad Prism software (version 4.03; GraphPad Software, Inc., La Jolla, CA). Single groups were compared by an unpaired two-tailed *t* test. Data were expressed as the mean ± SEM. Statistical significance was assumed at a P value of < 0.05.

ACKNOWLEDGMENTS

The authors thank Dan Draganovic and Janina Mandelbaum for their expert technical assistance.

This work was supported by grants from the Deutsche Forschungsgemeinschaft (AN372/11-1 and GRK1202 to H.-J.A. and LE2621/2-1 to M.L). Parts of this work were performed as a medical thesis by R.G. at the Medical Faculty of the University of Munich. R.G. was funded by the FöFoLe program of the Medical Faculty of the University of Munich.

DISCLOSURES

None.

REFERENCES

1. Briggs JD, Kennedy AC, Young LN, Luke RG, Gray M: Renal function after acute tubular necrosis. *BMJ* 3: 513–516, 1967
2. Goldstein SL, Devarajan P: Acute kidney injury in childhood: Should we be worried about progression to CKD? *Pediatr Nephrol* 26: 509–522, 2011
3. Ishani A, Xue JL, Himmelfarb J, Eggers PW, Kimmel PL, Molitoris BA, Collins AJ: Acute kidney injury increases risk of ESRD among elderly. *J Am Soc Nephrol* 20: 223–228, 2009
4. Dikow R, Becker LE, Schaier M, Waldherr R, Gross ML, Zeier M: In renal transplants with delayed graft function chemokines and chemokine receptor expression predict long-term allograft function. *Transplantation* 90: 771–776, 2010
5. Coca SG, Singanamala S, Parikh CR: Chronic kidney disease after acute kidney injury: A systematic review and meta-analysis. *Kidney Int* 81: 442–448, 2012
6. Lo LJ, Go AS, Chertow GM, McCulloch CE, Fan D, Ordoñez JD, Hsu CY: Dialysis-requiring acute renal failure increases the risk of progressive chronic kidney disease. *Kidney Int* 76: 893–899, 2009
7. Rifkin DE, Coca SG, Kalantar-Zadeh K: Does AKI truly lead to CKD? *J Am Soc Nephrol* 23: 979–984, 2012
8. Hsu CY: Yes, AKI truly leads to CKD. *J Am Soc Nephrol* 23: 967–969, 2012
9. Bonventre JV, Yang L: Cellular pathophysiology of ischemic acute kidney injury. *J Clin Invest* 121: 4210–4221, 2011
10. Abuelo JG: Normotensive ischemic acute renal failure. *N Engl J Med* 357: 797–805, 2007
11. Anders HJ: Toll-like receptors and danger signaling in kidney injury. *J Am Soc Nephrol* 21: 1270–1274, 2010
12. Allam R, Scherbaum CR, Darisipudi MN, Mulay SR, Hägele H, Lichtnekert J, Hagemann JH, Rupanagudi KV, Ryu M, Schwarzenberger C, Hohenstein B, Hugo C, Uhl B, Reichel CA, Krombach F, Monestier M, Liapis H, Moreth K, Schaefer L, Anders HJ: Histones from dying renal cells aggravate kidney injury via TLR2 and TLR4. *J Am Soc Nephrol* 23: 1375–1388, 2012
13. Wu H, Ma J, Wang P, Corpuz TM, Panchapakesan U, Wyburn KR, Chadban SJ: HMGB1 contributes to kidney ischemia reperfusion injury. *J Am Soc Nephrol* 21: 1878–1890, 2010

14. Wu H, Chen G, Wyburn KR, Yin J, Bertolino P, Eris JM, Alexander SI, Sharland AF, Chadban SJ: TLR4 activation mediates kidney ischemia/reperfusion injury. *J Clin Invest* 117: 2847–2859, 2007
15. Leemans JC, Stokman G, Claessen N, Rouschop KM, Teske GJ, Kirschning CJ, Akira S, van der Poll T, Weening JJ, Florquin S: Renal-associated TLR2 mediates ischemia/reperfusion injury in the kidney. *J Clin Invest* 115: 2894–2903, 2005
16. Iyer SS, Pulskens WP, Sadler JJ, Butter LM, Teske GJ, Ulland TK, Eisenbarth SC, Florquin S, Flavell RA, Leemans JC, Sutterwala FS: Necrotic cells trigger a sterile inflammatory response through the Nlrp3 inflammasome. *Proc Natl Acad Sci U S A* 106: 20388–20393, 2009
17. Anders HJ, Muruve DA: The inflammasomes in kidney disease. *J Am Soc Nephrol* 22: 1007–1018, 2011
18. Anders HJ, Vielhauer V, Schlöndorff D: Chemokines and chemokine receptors are involved in the resolution or progression of renal disease. *Kidney Int* 63: 401–415, 2003
19. Swaminathan S, Griffin MD: First responders: Understanding monocyte-lineage traffic in the acutely injured kidney. *Kidney Int* 74: 1509–1511, 2008
20. Anders HJ, Ryu M: Renal microenvironments and macrophage phenotypes determine progression or resolution of renal inflammation and fibrosis. *Kidney Int* 80: 915–925, 2011
21. Zhang MZ, Yao B, Yang S, Jiang L, Wang S, Fan X, Yin H, Wong K, Miyazawa T, Chen J, Chang I, Singh A, Harris RC: CSF-1 signaling mediates recovery from acute kidney injury. *J Clin Invest* 122: 4519–4532, 2012
22. Lee S, Huen S, Nishio H, Nishio S, Lee HK, Choi BS, Ruhrberg C, Cantley LG: Distinct macrophage phenotypes contribute to kidney injury and repair. *J Am Soc Nephrol* 22: 317–326, 2011
23. Ko GJ, Boo CS, Jo SK, Cho WY, Kim HK: Macrophages contribute to the development of renal fibrosis following ischaemia/reperfusion-induced acute kidney injury. *Nephrol Dial Transplant* 23: 842–852, 2008
24. Yang L, Besschetnova TY, Brooks CR, Shah JV, Bonventre JV: Epithelial cell cycle arrest in G2/M mediates kidney fibrosis after injury. *Nat Med* 16**:** 535–543, 1 p following 143, 2010
25. Mulay SR, Thomasova D, Ryu M, Anders HJ: MDM2 (murine double minute-2) links inflammation and tubular cell healing during acute kidney injury in mice. *Kidney Int* 81: 1199–1211, 2012
26. Price PM, Safirstein RL, Megyesi J: The cell cycle and acute kidney injury. *Kidney Int* 76: 604–613, 2009
27. Martin P, Leibovich SJ: Inflammatory cells during wound repair: The good, the bad and the ugly. *Trends Cell Biol* 15: 599–607, 2005
28. Furuichi K, Kaneko S, Wada T: Chemokine/chemokine receptor-mediated inflammation regulates pathologic changes from acute kidney injury to chronic kidney disease. *Clin Exp Nephrol* 13: 9–14, 2009
29. Takeuchi O, Akira S: Pattern recognition receptors and inflammation. *Cell* 140: 805–820, 2010
30. Suzuki N, Suzuki S, Duncan GS, Millar DG, Wada T, Mirtsos C, Takada H, Wakeham A, Itie A, Li S, Penninger JM, Wesche H, Ohashi PS, Mak TW, Yeh WC: Severe impairment of interleukin-1 and Toll-like receptor signalling in mice lacking IRAK-4. *Nature* 416: 750–756, 2002
31. Kobayashi K, Hernandez LD, Galán JE, Janeway CA Jr, Medzhitov R, Flavell RA: IRAK-M is a negative regulator of Toll-like receptor signaling. *Cell* 110: 191–202, 2002
32. del Fresno C, Otero K, Gómez-García L, González-León MC, Soler-Ranger L, Fuentes-Prior P, Escoll P, Baos R, Caveda L, García F, Arnalich F, López-Collazo E: Tumor cells deactivate human monocytes by up-regulating IL-1 receptor associated kinase-M expression via CD44 and TLR4. *J Immunol* 174: 3032–3040, 2005
33. Deng JC, Cheng G, Newstead MW, Zeng X, Kobayashi K, Flavell RA, Standiford TJ: Sepsis-induced suppression of lung innate immunity is mediated by IRAK-M. *J Clin Invest* 116: 2532–2542, 2006
34. Hotchkiss RS, Strasser A, McDunn JE, Swanson PE: Cell death. *N Engl J Med* 361: 1570–1583, 2009
35. Lech M, Kantner C, Kulkarni OP, Ryu M, Vlasova E, Heesemann J, Anz D, Endres S, Kobayashi KS, Flavell RA, Martin J, Anders HJ: Interleukin-1 receptor-associated kinase-M suppresses systemic lupus erythematosus. *Ann Rheum Dis* 70: 2207–2217, 2011
36. Li H, Cuartas E, Cui W, Choi Y, Crawford TD, Ke HZ, Kobayashi KS, Flavell RA, Vignery A: IL-1 receptor-associated kinase M is a central regulator of osteoclast differentiation and activation. *J Exp Med* 201: 1169–1177, 2005
37. Stearns-Kurosawa DJ, Osuchowski MF, Valentine C, Kurosawa S, Remick DG: The pathogenesis of sepsis. *Annu Rev Pathol* 6: 19–48, 2011
38. van 't Veer C, van den Pangaart PS, van Zoelen MA, de Kruif M, Birjmohun RS, Stroes ES, de Vos AF, van der Poll T: Induction of IRAK-M is associated with lipopolysaccharide tolerance in a human endotoxemia model. *J Immunol* 179: 7110–7120, 2007
39. Biswas SK, Lopez-Collazo E: Endotoxin tolerance: New mechanisms, molecules and clinical significance. *Trends Immunol* 30: 475–487, 2009
40. Seki M, Kohno S, Newstead MW, Zeng X, Bhan U, Lukacs NW, Kunkel SL, Standiford TJ: Critical role of IL-1 receptor-associated kinase-M in regulating chemokine-dependent deleterious inflammation in murine influenza pneumonia. *J Immunol* 184: 1410–1418, 2010
41. Zeisberg M, Neilson EG: Mechanisms of tubulointerstitial fibrosis. *J Am Soc Nephrol* 21: 1819–1834, 2010
42. Wynn TA, Ramalingam TR: Mechanisms of fibrosis: Therapeutic translation for fibrotic disease. *Nat Med* 18: 1028–1040, 2012
43. Mantovani A, Sica A, Sozzani S, Allavena P, Vecchi A, Locati M: The chemokine system in diverse forms of macrophage activation and polarization. *Trends Immunol* 25: 677–686, 2004
44. Ryu M, Kulkarni OP, Radomska E, Miosge N, Gross O, Anders HJ: Bacterial CpG-DNA accelerates Alport glomerulosclerosis by inducing an M1 macrophage phenotype and tumor necrosis factor-α-mediated podocyte loss. *Kidney Int* 79: 189–198, 2011
45. Famulski KS, Reeve J, de Freitas DG, Kreepala C, Chang J, Halloran PF: Kidney transplants with progressing chronic diseases express high levels of acute kidney injury transcripts. *Am J Transplant* 13: 634–644, 2013
46. Wang Y, Wang YP, Zheng G, Lee VW, Ouyang L, Chang DH, Mahajan D, Coombs J, Wang YM, Alexander SI, Harris DC: Ex vivo programmed macrophages ameliorate experimental chronic inflammatory renal disease. *Kidney Int* 72: 290–299, 2007
47. Lassen S, Lech M, Römmele C, Mittruecker HW, Mak TW, Anders HJ: Ischemia reperfusion induces IFN regulatory factor 4 in renal dendritic cells, which suppresses postischemic inflammation and prevents acute renal failure. *J Immunol* 185: 1976–1983, 2010
48. Lech M, Avila-Ferrufino A, Allam R, Segerer S, Khandoga A, Krombach F, Garlanda C, Mantovani A, Anders HJ: Resident dendritic cells prevent postischemic acute renal failure by help of single Ig IL-1 receptor-related protein. *J Immunol* 183: 4109–4118, 2009
49. Garlanda C, Anders HJ, Mantovani A: TIR8/SIGIRR: an IL-1R/TLR family member with regulatory functions in inflammation and T cell polarization. *Trends Immunol* 30: 439–446, 2009
50. Gurtner GC, Werner S, Barrandon Y, Longaker MT: Wound repair and regeneration. *Nature* 453: 314–321, 2008
51. Lech M, Anders HJ: Macrophages and fibrosis: How resident and infiltrating mononuclear phagocytes orchestrate all phases of tissue injury and repair. *Biochim Biophys Acta* 1832: 989–997, 2013
52. Ricardo SD, van Goor H, Eddy AA: Macrophage diversity in renal injury and repair. *J Clin Invest* 118: 3522–3530, 2008
53. Weidenbusch M, Anders HJ: Tissue microenvironments define and get reinforced by macrophage phenotypes in homeostasis or during inflammation, repair and fibrosis. *J Innate Immun* 4: 463–477, 2012
54. Dehmel S, Wang S, Schmidt C, Kiss E, Loewe RP, Chilla S, Schlöndorff D, Gröne HJ, Luckow B: Chemokine receptor Ccr5 deficiency induces alternative macrophage activation and improves long-term renal allograft outcome. *Eur J Immunol* 40: 267–278, 2010

55. Lech M, Römmele C, Gröbmayr R, Eka Susanti H, Kulkarni OP, Wang S, Gröne HJ, Uhl B, Reichel C, Krombach F, Garlanda C, Mantovani A, Anders HJ: Endogenous and exogenous pentraxin-3 limits post-ischemic acute and chronic kidney injury. *Kidney Int* 83: 647–661, 2013
56. Ninichuk V, Clauss S, Kulkarni O, Schmid H, Segerer S, Radomska E, Eulberg D, Buchner K, Selve N, Klussmann S, Anders HJ: Late onset of Ccl2 blockade with the Spiegelmer mNOX-E36-3'PEG prevents glomerulosclerosis and improves glomerular filtration rate in db/db mice. *Am J Pathol* 172: 628–637, 2008
57. Lech M, Susanti HE, Römmele C, Gröbmayr R, Günthner R, Anders HJ: Quantitative expression of C-type lectin receptors in humans and mice. *Int J Mol Sci* 13: 10113–10131, 2012

See related editorial, "Macrophage Dynamics in AKI to CKD Progression," on pages 209–211.

This article contains supplemental material online at http://jasn.asnjournals.org/lookup/suppl/doi:10.1681/ASN.2013020152/-/DCSupplemental.